

Melting MHD Stagnation Point Flow and Heat Transfer of a Nano fluid with Non-linear Thermal Radiation and Chemical Reaction

Kemparaju M. C¹, B. Lavanya², Mahantesh M. Nandeppanavar³, N. Raveendra⁴

¹Department of Mathematics, Jyothi Institute of Technology, Bangalore, India

²Department of Mathematics, Manipal Institute of Technology, MAHE, Manipal, India

³Department of Mathematics, Government College (Autonomous), Kalaburagi, India

⁴Department of Mathematics, Rajarajeswari College of Engineering, Bangalore, India

²lavanya.b@manipal.edu

ABSTRACT

The two-dimensional limit layer stream of the Liquefying MHD stagnation point stream and warmth movement of a Nano liquid with non-direct warm radiation and compound reaction was researched in the current paper. The supervising PDE's are turned into an arrangement of Tribute's using rational adjustments in likeness and then mathematically unravelled using shooting strategy. The effect on speed, temperature and concentrate profiles of dissolving heat action, Prandtl number, material reaction, warm radiation and Schmidt number, similar to bountiful significant boundaries, is studied graphically

Keywords

Heat transfer, Nano fluid, Chemical reaction, Thermal radiation

Article Received: 10 August 2020, Revised: 25 October 2020, Accepted: 18 November 2020

Introduction

In fluid components, a stagnation point is a point in a stream field where the local speed of the fluid is zero. Stagnation centers exist at the outside of articles in the stream field, where the fluid is brought to rest by the thing. Dinarvand et al. [1] developed the likeness answer for the MHD volatile stagnation point stream with delicacy sway. Accordingly, the volumetric segment of nanoparticles is nearly the essential variable for a given nanofluid that expects job in the progression of temperature and speed fields just as the essential measures of configuration interest. In this article, to specifically concentrate on the stagnation point stream of copper/water Nano liquids, a contemporary and sensible Nano liquid model is used. In [2], the model was developed. Bachok et al.[3] are inspecting the two-dimensional stagnation lead stream of gooey liquid to a convectively warmed extending/contracting layer. Hayat et al.[4], for example, considered the stagnation point stream of second grade liquid over an expanding warmth and mass exchange surface. This model provides detailed data for some practical Nano liquids, like Cu/water, which are considered to be a promising Nano liquid for hot applications in the related companies. Accordingly, With regard to this specific category of Nano liquids, the writing involves several trial attempts, mainly studying the convective warmth movement in pipes/tubes in both laminar and tempestuous structures (see, e.g.,[5-7]). Nandeppanavar, et.al[8] Non-Newtonian fluid stagnation point stream and warmth pass in a permeable medium over an extending/contracting layer. Dissolving heat move investigation of non-Newtonian Casson liquid due to moving plate was considered by Mahantesh .M [9].

The storey definition of "nanofluids" has been suggested as a way to outperform the presentation of flowing liquids of warmth as now available. When continuously spread and

gradually suspended in base liquids, a modest quantity of nanoparticles will provide notable improvements in the warm properties of base liquids. Rashidi et al.[10] used the second thermodynamic rule to use nanofluids, which are a colloidal mixture of nanoparticles (1–100 nm) and a base fluid (nanoparticle liquid suspensions). With the concept of different types of nanoparticles, to report the entropy age for the turning nanofluid stream crisis. Nadeem et al.[11] addressed the turning liquid stream problem concerning nanoparticles of copper and titanium oxide and found that fluctuating estimates of the volume of nanoparticle decrease the speed of nanoparticles. The effect of Brownian motion and thermophoresis on the pivoting nanofluid stream influenced by attractive, radiation, heat source and gooey dispersal impacts was studied by Mabood et al.[12]. Das et al.[13] studied the combined effect of attractive field and revolution in gooey liquid's transient hydromagnetic Couette stream and owing to these impacts, tremendous alteration in liquid speed was achieved. In order to investigate the influence of attractive and dense dispersion on the hydro attractive Couette stream in a pivoting system, Ali et al.[14] considered different forms of nanoparticle.

In every synthetic cycle, the mechanism of mass exchange is primarily important for the species whose fixation differs. Under these conditions, species growth is separated from a low-focus locale to a high-fixation territory.

Due to its gigantic applications such as geothermal stores, atomic reactor cooling and hot oil recovery, mass-heat movement instrument by material measurements has become a field of concern for specialists. In synthetic nature, geothermal and water and oil emulsion mechanics, the uses of enactment energy are altered. Within the sight of warmth age/retention, T.suatha et al.[15] introduced nonlinear implications for MHD nanofluid stream beyond expanding layer. B. Zigta[16] considered the influence of warm radiation and synthetic reaction on the MHD stream of blood in the porous vessel extension. Impact of compound

reaction and dual delineation on warmth and mass exchange attributes of nanofluid stream over permeable expanding layer with warm radiation is considered by P. Sudarsana Reddy et.al[17]. The effect of material calculation on the Burgers liquid 3D stream was dissected by Khan et al.[18]. The effect of synthetic response on summed-up Burgers liquid by using the nanoparticles was investigated by Khan et al.[19]. Mustafa et al.[20] inspected the magneto-nanofluid qualities of the initiation energy and material system. Pop B.L Ioan et. Al.[21] considered a nanofluid's point stream and warmth movement through an extending/contracting sheet with liquefying, convective warmth movement and second request slip and wubshet Ibrahim[22] considered a nanofluid's MHD maximum layer stagnation point stream and a nanofluid's warmth movement past a dissolving extending sheet. We have established our current paper in light of these papers. M.Nandeeshappanar et.al[23] considered the heat flow of hot radiative MHD stagnation point slip stream due to an expanding layer. Because of a nonlinear motion surface with the influence of a non-uniform source of warmth, M.Nandeeshappanar et.al[24] considered MHD stagnation point slip stream. B. Lavanya et.al[25] investigated the warmth and mass exchange of an MHD stream of a nanofluid in an annular, round district with external fluid through a permeable medium Chamber Kept up at Consistent Warmth motion. No research that talks about the two-dimensional limit layer stream of Softening MHD stagnation point stream and warmth step of a Nano liquid with non-direct warm radiation and synthetic reaction has been accounted for to the best of creator knowledge. Therefore this analysis is based on filling this knowledge void. The administration of PDE's is turned into a scheme of Tribute's using logical improvements in likeness and then mathematically unravelled by using the shooting method. The effect on speed, temperature and fixation profiles of dissolving heat movement, Prandtl number, material reaction, and warm radiation and Schmidt number, comparable to abundant significant boundaries, is graphically investigated.

Mathematical Formulation

It explores a two-dimensional consistent state MHD stagnation point limit layer stream and a nanofluid's warmth movement past an expanding sheet that softens into a steady property at a consistent rate. The stream is exposed to clear cross over appealing solidarity area $P = P_0$ which is applied typical of the sheet in the positive y-course

$$\frac{\partial m}{\partial x} + \frac{\partial n}{\partial y} = 0 \tag{1}$$

$$m \frac{\partial m}{\partial x} + n \frac{\partial n}{\partial y} = n \frac{\partial^2 n}{\partial y^2} + U_\infty \frac{\partial U_\infty}{\partial x} + \frac{\sigma p_0^2}{\rho_f} (U_\infty - m) \tag{2}$$

$$m \frac{\partial T}{\partial x} + n \frac{\partial T}{\partial y} = \alpha \frac{\partial^2 T}{\partial y^2} + \tau \left\{ D_B \frac{\partial c}{\partial y} \frac{\partial T}{\partial y} + \frac{D_B}{T_\infty} \left(\frac{\partial T}{\partial y} \right)^2 \right\} - \frac{1}{\rho c_p} \frac{\partial q_r}{\partial y} \tag{3}$$

$$m \frac{\partial R}{\partial y} + n \frac{\partial R}{\partial y} = D_B \frac{\partial^2 R}{\partial y^2} + \frac{D_B}{T_\infty} \frac{\partial^2 T}{\partial y^2} - K_r (R - R_\infty) \tag{4}$$

Where $\alpha = \frac{k}{(\rho R)_f}$, $\tau = \frac{(\rho R)_p}{(\rho R)_f}$

For the current investigation, limit conditions recommended are

$$m = m_w = cx, \quad n = 0, \quad T = T_m, \quad R = R_w \text{ at } y = 0$$

$$m \rightarrow U_\infty = dx, \quad n = 0, \quad T \rightarrow T_\infty, \quad R \rightarrow R_\infty \text{ as } y \rightarrow \infty$$

$$\alpha \left(\frac{\partial T}{\partial y} \right)_{y=0} = \rho [\lambda + C_s (T_m - T_0)] n(x, 0) \tag{5}$$

Under Roseland estimation, the radiative warmth transition

Q_r is taken in the structure

$$q_r = - \frac{4\sigma^* \partial T^4}{3k^* \partial y} \tag{6}$$

Here σ^* , k^* are Stefan–Boltzman steady and mean assimilation coefficient separately. This examination accepts hotness contrasts inside the stream T^4 are with the end goal that might be expressed as a straight mix of the temperature.

We grow T^4 in a Taylor's arrangement T_∞ about and overlooking the higher request terms, we get

$$T^4 \cong 4T_\infty^3 T - 3T_\infty^4 \tag{7}$$

On utilizing Eq. (7) in Eq. (6) we accomplish

$$\frac{\partial q_r}{\partial y} = - \frac{16T_\infty^3 \sigma^* \partial^2 T}{3k^* \partial y^2} \tag{8}$$

Allow us to characterize the comparability variable (η) and the dimensionless factors in wording similitude factors

$$\eta = y \sqrt{\frac{a}{\nu}}, \quad \psi = \sqrt{av} \alpha(\eta), \quad \beta(\eta) = \frac{T - T_m}{T_\infty - T_m}, \quad \gamma(\eta) = \frac{R - R_\infty}{R_w - R_\infty} \tag{9}$$

The condition of coherence is fulfilled in the event that we pick a stream work $\psi(x,y)$ with the end goal that

$$m = \frac{\partial \psi}{\partial y}, \quad n = - \frac{\partial \psi}{\partial x} \tag{10}$$

Utilizing the closeness change amounts condition (9), the overseeing conditions (1)- (4) are changed into the non-dimensional structure as follows

$$\alpha''' + \alpha\alpha'' - \alpha'^2 + A^2 + M(A - \alpha') = 0 \tag{11}$$

$$(1 + N_r(1 + (\beta_w - 1)\beta)^2 \beta') + Pr(\alpha\beta' + N_b\gamma'\beta\beta' + Nt\beta\beta'') = 0 \tag{12}$$

$$\gamma'' + PrLef\beta' + \frac{Nt}{Nb}\beta'' - Sc\lambda\gamma = 0 \tag{13}$$

The parallel boundary situations are

$$\alpha'(0) = 1, \quad P\beta'(0) + Pr\alpha(0) = 0, \quad \beta(0) = 0, \quad \gamma(0) = 1$$

at $y = 0$

$$\alpha'(\infty) = A, \quad \beta(\infty) = 1, \quad \gamma(\infty) = 0 \text{ at } y \rightarrow \infty \tag{14}$$

Where the main requirements are characterized by

$$M = \frac{\sigma B_0^2}{\rho_f \alpha}, \quad Le = \frac{\alpha}{D_B}, \quad Pr = \frac{m}{\alpha}, \quad A = \frac{d}{c}, \quad N_r = \frac{16\sigma T_m^3}{3kk^*}, \quad \delta = \frac{K_r}{c}$$

$$Nb = \frac{(\rho c)_p D_B (\theta_B - \theta_\infty)}{(\rho c)_f \alpha}, \quad Nt = \frac{(\rho c)_p D_T (T_w - T_\infty)}{(\rho c)_f \alpha T_\infty}, \quad P = \frac{C_f (T_\infty - T_m)}{\lambda + C_s (T_m - T_0)} \tag{15}$$

Where α, β and γ are the dimensionless velocity, temperature and concentration respectively. B is the dimensionless melting parameter which is defined by $P = \frac{C_f (T_\infty - T_m)}{\lambda + C_s (T_m - T_0)}$ and it is a combination of the Stefan numbers $\frac{C_f (T - T_0)}{\lambda}$ for the liquid and solid phases, respectively.

In light of the above amounts, the skin grinding coefficient C_f the local Nusselt number Nu_x and the neighborhood Sherwood number Sh_x characterized as

$$C_f = \frac{\tau_w}{\rho u_w^2}, Nu_x = \frac{xq_w}{k(T_\infty - T_m)}, Sh_x = \frac{xh_m}{D_B(R_w - R_\infty)} \quad (16)$$

Where the wall shear stress τ_w , the wall heat flux q_w and wall mass flux h_m are given by

$$\tau_w = \mu \frac{\partial u}{\partial y}, q_w = \left(-k \left(\frac{\partial T}{\partial y} \right) + q_r \right)_{y=0}, h_m = -D_B \left(\frac{\partial C}{\partial y} \right)_{y=0} \quad (17)$$

By utilizing the above conditions, we get

$$C_f \sqrt{Re_x} = -\alpha''(0), \frac{Nu_x}{\sqrt{Re_x}} = -(1 + R\beta_w^2)\beta'(0), \frac{Sh_x}{\sqrt{Re_x}} = -\gamma'(0) \quad (18)$$

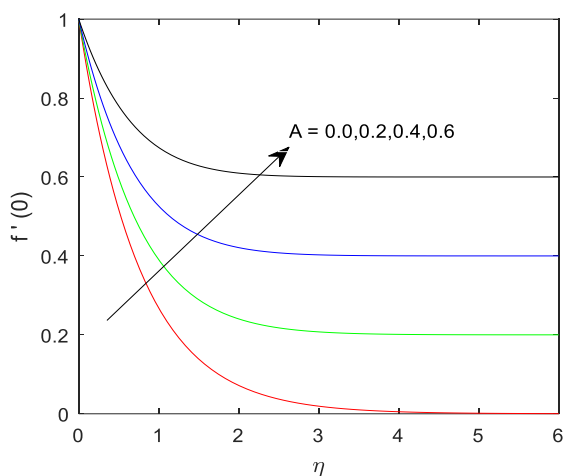


Fig. 1: Velocity profile for different values of A with $Le = 2, Pr = 1, B = 0.5, Nt = Nb = 0.3, M = 0.3, \theta_w = 1.1, \gamma = 0.1$ and $N_r = 1$

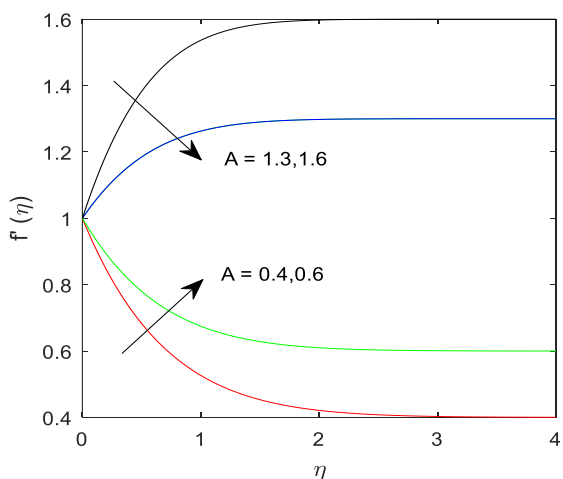


Fig. 2: Velocity profile for different values of A with $Le = 2, Pr = 1, B = 0.5, Nt = Nb = 0.3, M = 0.3, \theta_w = 1.1, \gamma = 0.1$ and $N_r = 1$

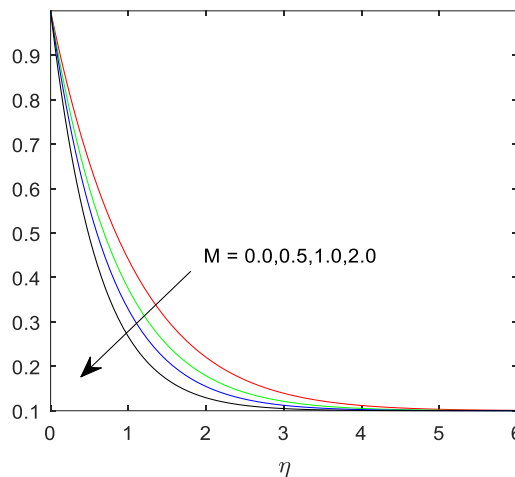


Fig. 4: Velocity profile for different values of M with $Le = 2, Pr = 1, B = 0.5, Nt = Nb = 0.3, A = 0.1, \theta_w = 1.1, \gamma = 0.1$ and $N_r = 1$

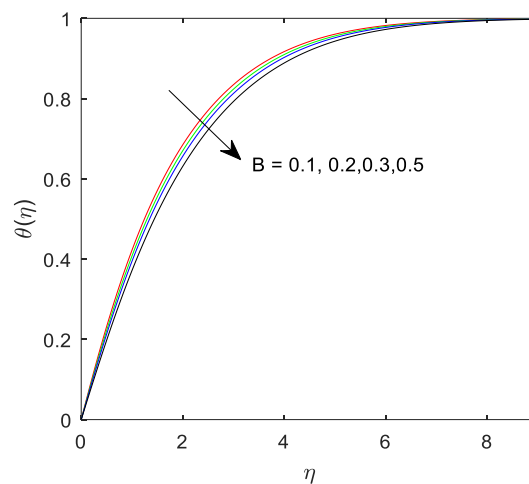


Fig. 5: Temperature profile for different values of B with $Le = 2, Pr = 1, M = 1, Nt = Nb = 0.3, A = 0.1, \theta_w = 1.1, \gamma = 0.1$ and $N_r = 1$

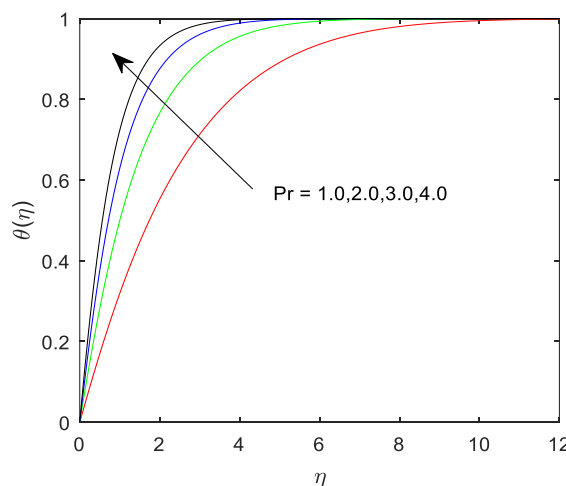


Fig. 6: Temperature profile for different values of Pr with $Le = 2, B = 0.5, M = 1, Nt = Nb = 0.3, A = 0.1, \theta_w = 1.1, \gamma = 0.1$ and $N_r = 1$

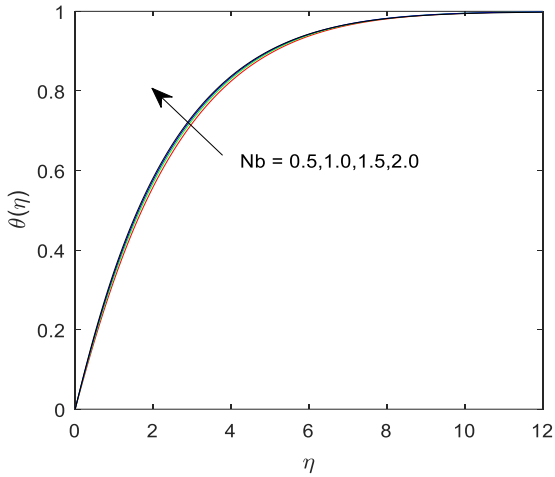


Fig. 7: Temperature profile for different values of Nb with $Le = 2, B = 0.5, M = 1, Pr = 1, Nt = 0.3, A = 0.1, \theta_w = 1.1, \gamma = 0.1$ and $N_r = 1$

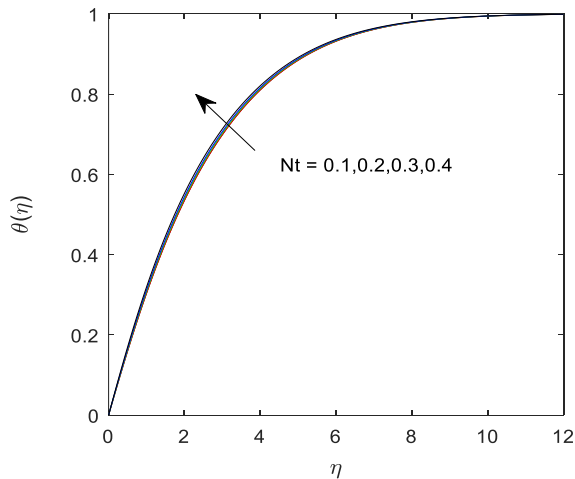


Fig. 8: Temperature profile for different values of Nt with $Le = 2, B = 0.5, M = 1, Pr = 1, Nb = 0.3, A = 0.1, \theta_w = 1.1, \gamma = 0.1$ and $N_r = 1$

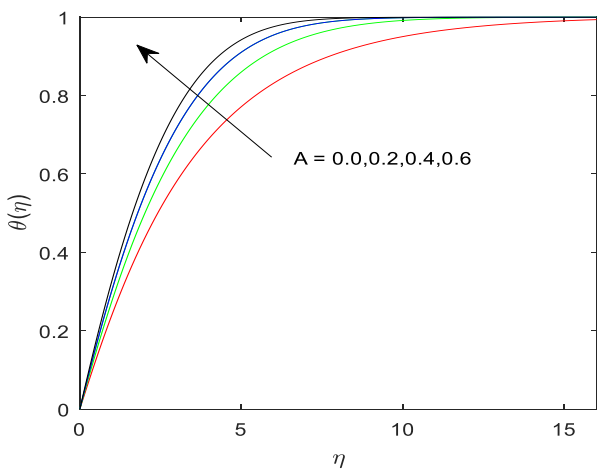


Fig. 9: Temperature profile for different values of A with $Le = 2, B = 0.5, M = 1, Pr = 1, Nb = Nt = 0.3, \theta_w = 1.1, \gamma = 0.1$ and $N_r = 1$

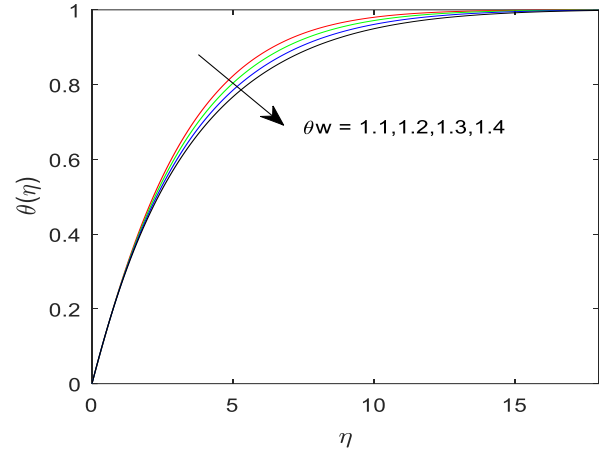


Fig. 11: Temperature profile for different values of θ_w with $Le = 2, B = 0.5, M = 1, Pr = 1, Nb = Nt = 0.3, A = 0.1, \gamma = 0.1$ and $N_r = 1$

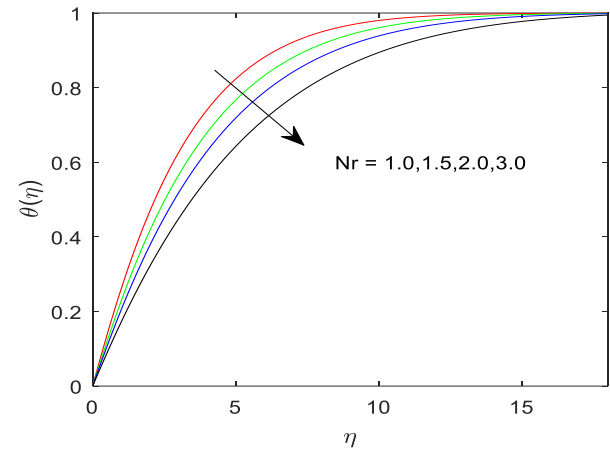


Fig. 12: Temperature profile for different values of N_r with $Le = 2, B = 0.5, M = 1, Pr = 1, Nb = Nt = 0.3, A = 0.1, \gamma = 0.1$ and $\theta_w = 1.1$

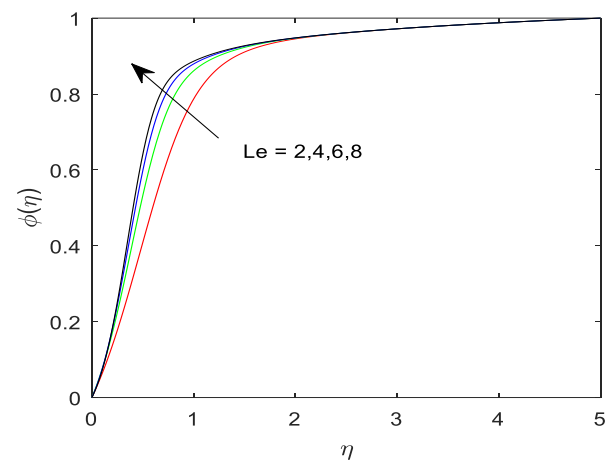


Fig. 13: Concentration Profile for different values of Le with $N_r = 1, B = 0.5, M = 0.3, Pr = 0.5, Nt = Nb = 0.5, \beta = 0.5, \theta_w = 1.1$ and $A = 0$.

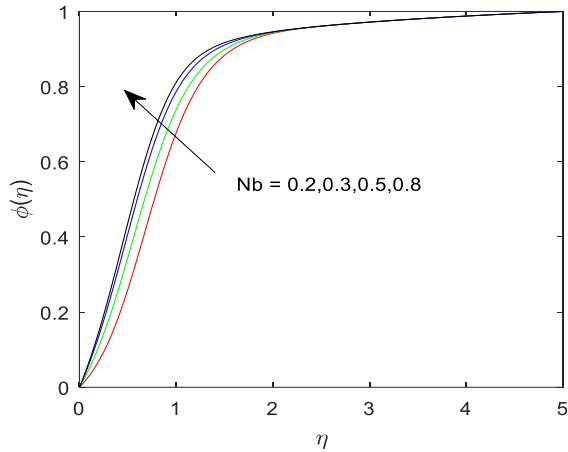


Fig. 14: Concentration Profile for different values of Nb with $Le = 2, N_r = 1, B = 0.5, M = 0.3, Pr = 0.5, Nt = 0.5, \beta = 0.5, \theta_w = 1.1$ and $A = 0.1$

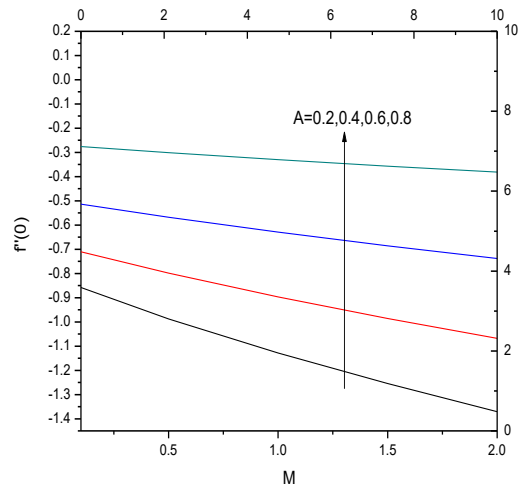


Fig. 17: Graph of skin friction coefficient $-f''(0)$ for different values of M along with velocity ratio parameter A when $Le = 2, Pr = 0.5, B = 0.5, Nt = Nb = 0.3, \gamma = 0.1, \theta_w = 1.1$ and $A = 0.1$

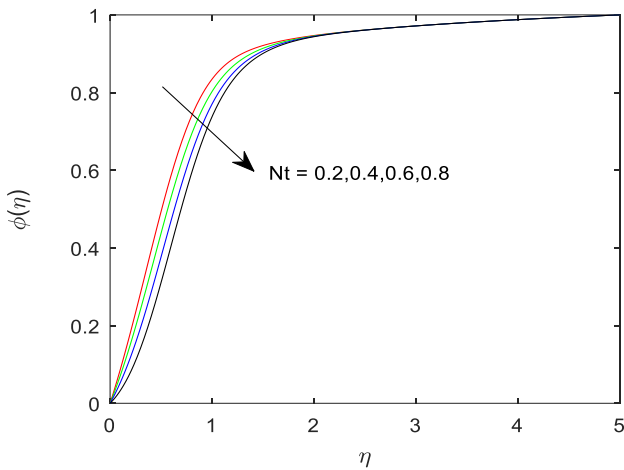


Fig. 15: Concentration Profile for different values of Nt with $Le = 2, N_r = 1, B = 0.5, M = 0.3, Pr = 0.5, Nb = 0.5, \gamma = 0.1, \theta_w = 1.1$ and $A = 0.1$

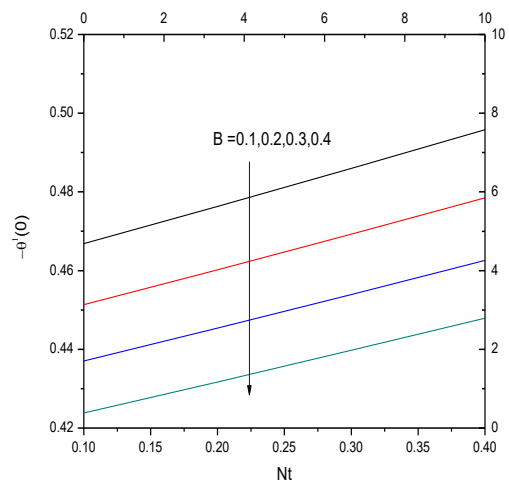


Fig. 18: Graph of local Nusselt number $\theta'(0)$ for different values of Nt along with melting heat transfer parameter B when $Le = 2, Pr = 0.5, Nb = 0.3, \gamma = 0.1, M = 1, \theta_w = 1.1, N_r = 1$

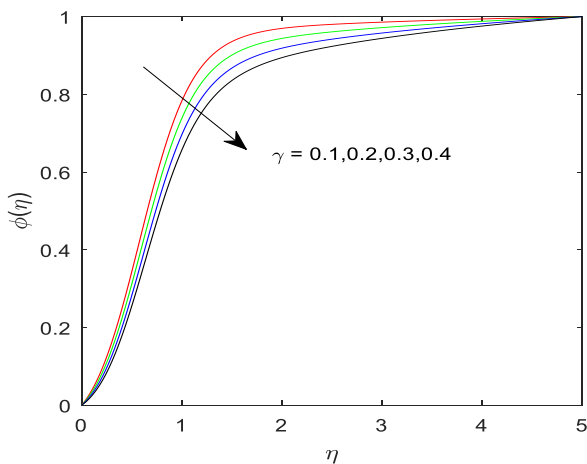


Fig. 16: Concentration Profile for different values of Nt with $Le = 2, N_r = 1, B = 0.5, M = 0.3, Pr = 0.5, Nt = Nb = 0.5, A = 0.1$ and $\theta_w = 1.1$

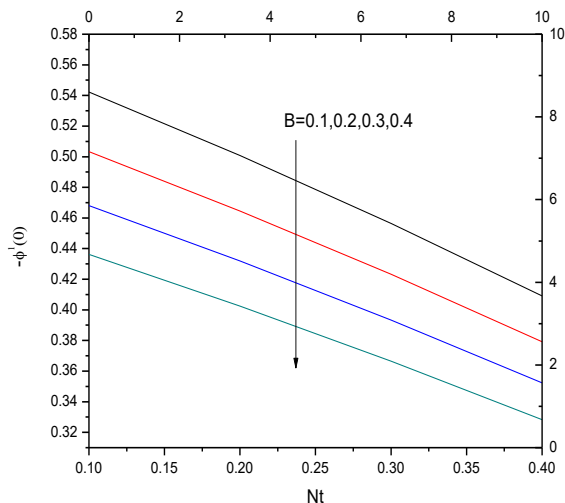


Fig. 19: Graph of local Sherwood number $\phi'(0)$ for different values of Nt along with melting heat transfer parameter B when $Le = 2, Pr = 0.5, Nb = 0.3, \gamma = 0.1, M = 1, \theta_w = 1.1, Nr = 1$ and $A = 0.2$

Validation of outcomes:

The actual effects of the unmistakable stream boundaries, for example, the speed proportion A , Casson boundary β , attractive boundary M , liquefying heat move B , Brownian movement Nb , Thermophoresis Nt are shown through graphical illustration. Figs. 1 and 2 portrays that the higher estimations of speed proportion boundary A make an improvement inside the speed appropriations and BLT. Fig. 3 shows the variety in speed conveyance for a few estimations of Casson boundary β . It is imagined from the bends of speed work decelerate by upgrading the estimations of β . The idea of the speed in cautious reaction of various attractive boundary M is shown in the Fig 4. It is visualized from the diagram increase in M stream speed diminishes. Fig. 5 is depicted to see the qualities of $\theta(\eta)$ regarding η for unmistakable B . Improvement in dissolving heat move B prompts decline in $\theta(\eta)$. Fig. 6 uncovers the stream idea of energy dispersion on the Prandtl number Pr . It is obvious that the energy bends contacts to in y pivot and the comparing BLT decelerates. Fig. 7 is effectively molding the development of temperature profile $\theta(\eta)$ because of Nb . Brownian movement boundary Nb prompts blasting in $\theta(\eta)$ identified with BLT are the outcomes. Fig. 8 is uncovered to look at the idea of temperature work on thermophoresis boundary Nt . We have imagined that, temperature capacities are upsurges for elevating estimations of Nt . Fig. 9 portrays attributes of $\theta(\eta)$ as for η in light of A . Velocity proportion boundary A prompts improvement in $\theta(\eta)$ relating to BLT are the results. Fig. 10 passes on about the attributes $\theta(\eta)$ concerning η because of β . Casson boundary β prompts decrease in BLT which shows diminish in temperature field. Fig. 11 depicts to know the embodiment of divider temperature θ_w on energy profile. An addition in θ_w , decelerates in bend thickness, which shows a decrease in energy profile. Fig. 12

characterizes the impact of Nr over energy dispersions. It is imagined from the figure that the stream temperature decreases with developing estimations of Nr . The impact of Lewis number Le on focus field is examined in fig. 13. It is visible that an inspiring Lewis number, the fixation work upsurges. Fig. 14 uncovers the result of $\phi(\eta)$ concerning η in light of Nb . Brownian movement boundary Nb prompts decline in fixation. Fig. 15 shows the Concentration Profile for different values of Nt its been seen that higher values of Nt reduces the concentration level. Fig. 16 depicts the Concentration Profile for different values of Nt it leads to decrease in concentration with the increase in γ .

Fig. 17 exhibits the impact of magnetic parameter M on the velocity distributions to see the nature of skin friction. It is clear that for higher values of M skin friction enhances. Fig. 18 shows the behavior of skin friction on temperature distributions with the influence of thermophoresis parameter Nt along with melting heat transfer B . It is perceived from the graph, higher values of Nt and B reduction in skin friction. Fig. 19 portrays the behavior of skin friction on the concentration profile for distinct values thermophoresis parameter Nt along with melting heat transfer B . It's been visualized from the graph, for several values of Nt and B shows decelerate in skin friction.

Conclusion

In this article investigates the Melting MHD limit layer stagnation point development and warmth move of a Nano liquid with Non-direct warm radiation. The current work broke down that an expansion of nonlinear warm radiation, smothers the pace of warmth move. The principle closing focuses are given underneath:

- The wall temperature θ_w on energy profile enhances, it shows reduction in energy transfer. The influence of A on $f'(\eta)$ with respect to η , for certain values of velocity ratio parameter A enhances. If we further increase leads to dual solutions.
- It is imagined that, the warmth transport rate decelerates and mass exchange rate quickens with the improve of Casson boundary.
- The speed profile decelerates with quickening attractive boundary.
- An elevating in thermophoresis boundary Nt , It is pictured that the fixation work improves.

Acknowledgment:

The author would like to express special thanks of gratitude to all who helped me to finish this work.

References

- [1] Dinarvand S, Doosthoseini A, Doosthoseini E, Rashidi MM. Series solutions for unsteady laminar MHD flow near forward stagnation point of an impulsively rotating and translating sphere in presence of buoyancy forces. *Nonlinear Anal* 2010;11:1159–69.
- [2] Corcione, M.: Empirical correlating equations for predicting the effective thermal conductivity and dynamic viscosity of nanofluids. *Energy Convers. Manag.* 52, 789–793 (2011)
- [3] Rosali H, Ishak A, Nazar R, Merkin JH, Pop I. The effect of unsteadiness on mixed convection boundary-layer stagnation-point flow over a vertical flat surface embedded in a porous medium. *Int J Heat Mass Transfer* 2014;77:147–56.
- [4] Hayat T, Anwar MS, Farooq M, Alsaedi A. MHD stagnation point flow of second grade fluid over a stretching cylinder with heat and mass transfer. *Int J Nonlinear Sci Numer Simul* 2014;1–12.
- [5] Khoshvaght-Aliabadi, M.; Hormozi, F.; Zamzamian, A.: Selfsimilar analysis of fluid flow, heat, and mass transfer at orthogonal nanofluid impingement onto a flat surface. *Heat Mass Transf.* 51, 423 (2015).
- [6] Khoshvaght-Aliabadi, M.; Alizadeh, A.: An experimental study of Cu–water nanofluid flow inside serpentine tubes with variable straight-section lengths. *Exp. Therm. Fluid Sci.* 61, 1–11 (2015).
- [7] El-Maghlany, W.M.; Hanafy, A.A.; Hassan, A.A.; El-Magid, M.A.: Experimental study of Cu–water nanofluid heat transfer and pressure drop in a horizontal double-tube heat exchanger. *Exp. Therm. Fluid Sci.* 78, 100–111 (2016).
- [8] Nandeppanavar, M.M. and Shilpa, M.J. (2016), “Stagnation point flow of Non-Newtonian fluid and heat transfer over a stretching/shrinking sheet in a porous medium”, *Chemical and Process Engineering Research*, Vol. 46, pp. 27-34.
- [9] Mahantesh .M Nandeppanavar studied Melting heat transfer analysis of non-Newtonian Casson fluid due to moving plate. *Engineering Computations* Vol. 35 No. 3, 2018 pp. 1301-1313 © Emerald Publishing Limited
- [10] M. M. Rashidi, S. Abelman, N. F. Mehr, Entropy generation in steady MHD flow due to a rotating porous disk in a nanofluid, *International Journal of Heat and Mass Transfer*, 62 (2013) 515–525.
- [11] S. Nadeem, A. U. Rehman, R. Mehmood, Boundary layer flow of rotating two phase nanofluid over a stretching surface, *Heat Transfer-Asian Research*, 45(3) (2016) 285-298
- [12] F. Mabood, S.M. Ibrahim, W. A. Khan, Framing the features of Brownian motion and thermophoresis on radiative nanofluid flow past a rotating stretching sheet with magnetohydrodynamics, *Results in Physics*, 6 (2016) 1015–1023.
- [13] S. Das, R.N. Jana, O.D. Makinde, Transient hydromagnetic reactive Transient hydromagnetic reactive Couette flow and heat transfer in a rotating frame of reference, *Alexandria Engineering Journal*, 55(1) (2016) 635-644.
- [14] A.O. Ali, O.D. Makinde, Y. Nkansah-Gyekye, Numerical study of unsteady MHD Couette flow and heat transfer of nanofluids in a rotating system with convective cooling, *International Journal of Numerical Methods for Heat & Fluid Flow*, 26(5) (2016) 1567-1579.
- [15] T.suatha k. ayaramireddy and J. Girish Kumar presented nonlinear effects on MHD nanofluid flow past stretching sheet in the presence of heat generation /absorption. *AIP Conference Proceedings* 2246, 020092 (2020).
- [16] B. Zigta studied Effect of Thermal Radiation and Chemical Reaction on MHD Flow of Blood in Stretching Permeable Vesse August 2020 *International Journal of Applied Mechanics and Engineering* 25(3):198-211

- [17] P. Sudarsana Reddy & P. Sreedevi studied Impact of chemical reaction and double characteristics of nanofluid flow over porous stretching sheet with thermal radiation. International journal of ambient energy 20 jan 2020
- [18] Khan, W.A.; Alshomrani, A.S.; Khan, M.: Assessment on characteristics of heterogeneous-homogeneous processes in threedimensional flow of Burgers fluid. Results Phys. 6, 772–779 (2016)
- [19] Khan, W.A.; Irfan, M.; Khan, M.; Alshomrani, A.S.; Alzahrani, A.K.; Alghamdi, M.S.: Impact of chemical processes on magneto nanoparticle for the generalized Burgers fluid. J. Mol. Liq. 234, 201–208 (2017)
- [20] Mustafa, M.; Khan, J.A.; Hayat, T.; Alsaedi, A.: Buoyancy effects on the MHD nanofluid flow past a vertical surface with chemical reaction and activation energy. Int. J. Heat Mass Transf. 108, 1340– 1346 (2017)
- [21] Ioan pop et. Al. studied MHD stagnation – point flow and heat transfer of a nanofluid over a stretching/shrinking sheet with melting, convective heat transfer and second order slip. www.emeraldinsight.com/0961-5539.htm
- [22] wubshet Ibrahim studied MHD boundary layer stagnation point flow and heat transfer of a nanofluid past a stretching sheet with melting. Propulsion and power research 2017;6 (3):214-222